ICAS 2016
30th Congress of the International Council of the Aeronautical Sciences
DCC, Daejeon, Korea ; September 25-30, 2016

OPTIMISATION OF A WING-BODY-TAIL CONFIGURATION WITH AN ALTERNATIVE LOW DRAG FUSELAGE AND BODY TRAILING EDGE

Smith, L.*, Craig, K.J.*, Meyer, J.P.*, and Spedding, G.R.**
***University of Pretoria, **University of Southern California**

Keywords: *fuselage, low-drag body, aerodynamic efficiency, design optimisation*

Abstract

A wing-body-tail (WBT) configuration is proposed without the conventional tailplane, allowing for new requirements for the aerodynamic shape of the fuselage. A shorter, low drag body can be employed with a deflector trailing edge (Kutta edge/KE) to modify the flow around the body so as to allow wing-body circulation to be more uniform. Initial experimental and numerical work indicates benefits from both the low drag body profiles, as well as the addition of the deflector plate. The design space for such a deflector plate for the proposed WBT has not been explored. Therefore, the purpose of this study was to use an optimisation procedure to vary the aftbody deflection and KE shape to produce an optimum aerodynamic efficiency (L/D). The geometry varies by changing the KE spread angle and length, and deflecting the aftbody to optimise the WBT at Reynolds numbers of $1x10^5$, with the wing at a fixed $\alpha = 6°$, to determine whether a unique combination of these three parameters exists. Finally, the body is replaced with a low drag body, F-57 and KE shapes and aftbody deflections are optimised again. This work indicates a greater sensitivity to KE spread to achieve the best L/D than the other design variables. However, at a higher KE spread, L/D is increasingly affected by the other two variables.

1 Introduction

New aircraft configurations are predominantly proposed in order to improve the aerodynamic efficiency of the current standard tube-and-wing model, which is unlikely to represent an optimum. Static longitudinal stability can be achieved through the main wing geometry [1], alleviating the fuselage from the requirement to carry a tailplane. Therefore, the requirements for fuselage design are reconsidered. Two proposed requirements are to reduce drag by replacing the long, tubular body with a shorter low drag body, and to provide some circulation control over the body and aftbody portions to restore the lift portion that is lost by the wing from the addition of the fuselage.

Low drag bodies (LDBs) are traditionally investigated as airships, missiles and submarines without appendages, such as wings and tails [2-8]. These LDBs are typically shorter and wider, with the nose contours shaped to delay transition and aftbody contours to prevent separation. An overall body geometry improvement leads to a reduction of the viscous drag components.

If a different, shorter body is employed, then it can be possible to modify the flow around that body so that the circulation distribution between the body and wings is much more uniform. The proposed wing-body-tail (WBT) configuration [9, 10] employs a modified trailing edge deflector flap to the fuselage aftbody, termed Kutta Edge (KE). The KE controls the rear stagnation point, and therefore the lift on the main body/fuselage, which is otherwise uncompromised from its primary function as the payload carrier. This leads to an induced drag reduction since the downwash distribution can return to that of an ideal wing.

Two previous studies [9-12] deal with the characteristics of the WBT. The WBT sub-components are generally selected as a shorter, wider body, without regards to exact contours, a flat plate trailing edge, and a NACA0012 wing

(*AR* = 6.67). First some particle image velocimetry (PIV) flow field analysis results for the WBT at aftbody deflection angles, δ, of 0, 2, 4, 6, and 8° were compared to the force balance measurements in an attempt to provide an indication of drag reduction sources [10]. Because of the lumped measurement of forces, it was not possible to identify the specific contributions of the various aerodynamic surfaces to the experimental global force coefficient. A computational fluid dynamics (CFD) study [11] used the commercial code STAR-CCM+ to predict various aerodynamic properties of the WBT. There was an increase in lift for increasing δ, which was even more pronounced when the KE was added, but the penalty of drag led to a maximum *L*/*D* to existing at around δ = 4°.

Smith et al., 2016 [12] investigated combinations of LDBs with the KE. When the KE was combined to a LDB, the width of the KE relative to the LDB geometry influenced the overall efficiency of the LDB-KE. However, no attempt was made to provide an optimal arrangement of the LDB-KE or to combine the LDB-KE with a wing.

Therefore, the purpose of this study was to first consider the original body [9, 10] and KE combination in isolation and compare these results to the WBT. The KE and aftbody geometry will be changed to achieve a maximum *L*/*D* for a fixed wing angle of attack, α = 6° and Re = 1x10^5. Some general guidelines about the combination within the WBT were considered before adding a LDB and estimating the sensitivity of this combination. The investigation does not take any stability aspects into account. It merely provides a guideline for further WBT investigations and optimisations to determine if there is a unique aftbody-KE design for an aerodynamically more efficient WBT.

2 Computational Model Implementation

2.1 Geometric Model, Solution Domain and Mesh Generation

The WBT is a short body with the body length, *l* divided by the maximum body diameter, *d* of 5.33, a NACA0012 wing with AR = 6.67 and a reduced chord length, *c*, of 0.074m, 1mm shorter than the experimental model [9, 10] (wings were made blunt for ease of meshing). The wing was modelled at an angle of attack, α of 6°, a tail spread angle, T_S of 30°, and a tail length, T_L/l of 1.08. The second model used the same wing and KE but replaced the body with the F-57 LDB with *l*/*d* = 4.75.

The WBT was modelled in a simplified cylindrical shape representing the octagonal Dryden wind tunnel test section [9, 10]. The simplified geometry had less than 0.25% influence on the force components. The solution domain was only one half of the full domain with a symmetry plane in the centre of the model. The WBT was positioned at 6*l* from the inlet plane of the flow domain and the outlet plane was stretched downstream at 18*l*. The diameter of the wind tunnel is 1.36m, and the full test section length of the CFD model is 8m as shown in Fig. 1a. The domain for the F-57 LDB-KE with a wing was also modelled as a half-cylinder with a diameter of 7.4m, with the model 4*l* from the inlet and 10*l* from the outlet with a full test section length of 17.5m (Fig. 1b).

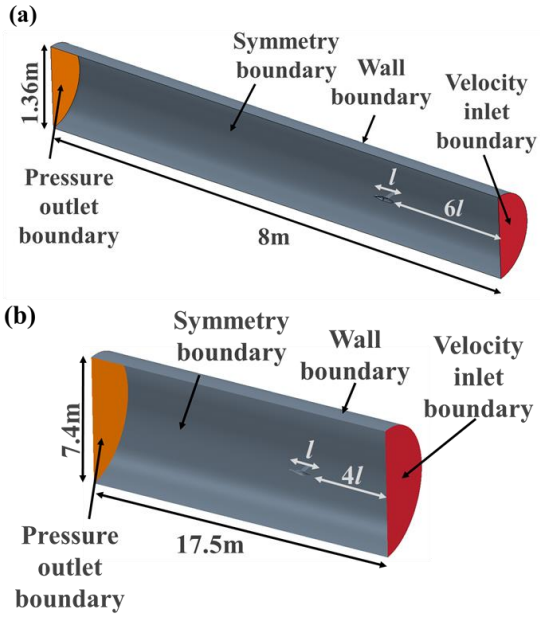

Fig. 1. Solution domain with boundary conditions for the WBT

The flow conditions were modelled as steady and incompressible, making use of a constant velocity inlet boundary condition, with Re = 1x10^5 based on *c* and the outlet pressure

boundary set at atmospheric conditions as shown in Fig.1a and b. The outer domains were modelled as no-slip wall boundaries.

All bodies were meshed using the same mesh functions and boundary layer mesh growth rate as [11, 12]. The WBT model had 15 boundary layer cells and two cells on the outer wall boundary were sufficient for force predictions. The volumetric mesh was subdivided in the same way as described in [11], but the refinements were less fine. Figure 2 shows the mesh around the WBT models.

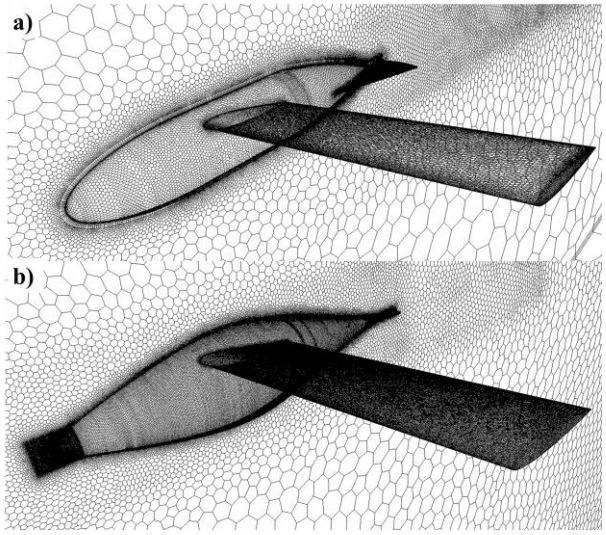

Fig. 2. Unstructured mesh around a) WBT and b) F-57

A mesh independence study on the most deflected aftbody angle (δ = 8°) model, confirms that the mesh count is adequate to capture the flow variables of interest. The Grid Convergence Index (GCI) method [13], was used on three different mesh sizes, to ensure that mesh independent grids were used. The final mesh counts for the WBT configuration was $2x10^6$ cells and for the F-57 $2.6x10^6$ cells and the criterion $y^+ < 1$ was satisfied in both cases.

2.2 Turbulence and Transition Models

The turbulence and transition models were selected as prescribed for aerospace application at low Re. The shear-stress transport (SST) k-ω turbulence model [14] coupled to γ-Re_θ transition model [15] was selected as in [11, 12]. The transition model is required for Re number (Re < 10^6) where laminar separation bubbles and transition become important to predict the aerodynamic forces with reasonable accuracy.

2.3 Optimisation

STAR-CCM+ /Enabling Optimate+ adds the capability to perform automated design optimisation studies coupled to the CFD simulations. The simultaneous hybrid exploration that is robust, progressive and adaptive (SHERPA) algorithm is embedded into the add-on and provides a best in class, easy to use and robust optimisation tool. SHERPA uses a combination of global and local search methods simultaneously, taking advantage of the best attributes of each method and reduces the search method's participation if the method is determined ineffective. Each method contains tuning parameters that are modified automatically during the search according to knowledge gained about the nature of the design space. The evolving knowledge about the design space also determines when and to what extent each method is being used. It has proven to be very effective and efficient for practical engineering problems [16].

3 Description of the Optimisation Study

The purpose of the optimisation study was to evaluate and comment on geometric sensitivities when considering the KE shape and aftbody deflections for WBT in terms of aerodynamic efficiency L/D. This served as a preliminary investigation where further detailed investigations will consider the underlying fluid mechanism responsible for these global force domain features.

In order to evaluate the influence of certain geometric changes, three variables were selected to optimise for L/D. Table 1 shows the initial geometric change values and number of intervals selected through which the geometric changes can occur. These changes were made in order to find the maximum L/D at body angle of 0° without any constraints applied. These three variables are illustrated in Fig. 3.

Geometric change	Conditions	Intervals
KE length (T_L/l)	$1.005 \leq T_L/l \leq 1.3$	0.005m
KE spread (T_S)	$4° \leq T_S \leq 30°$	2°
Aftbody angle (δ)	$0° \leq \delta \leq 8°$	1°

Table 1. Geometric changes applied during the optimisation simulation

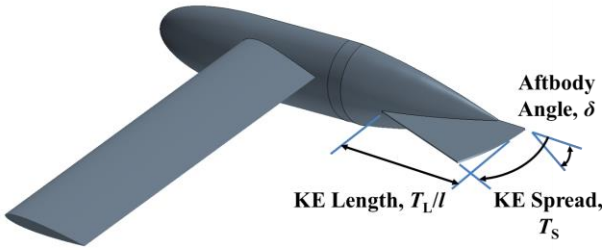

Fig. 3. Schematic of the geometric changes applied during the optimisation simulation

3.1 Optimisation Test Cases

The initial optimisation case study had a fixed wing position (α = 6°) and only varied the KE geometry (T_L/l and T_S) and δ. The relationship between these three parameters in terms of ideal L/D was evaluated in terms of the global forces and was also compared to the lift coefficient, C_L of a NACA0012 wing without the body and KE sections at α = 6°.

The second optimisation case study substituted the F-57 LDB into the WBT to determine whether the sensitivities remained the same for T_L/l, T_S and δ.

3.2 Sensitivity Study

3.2.1 Prior investigations on the proposed wing-body-tail configuration

The WBT configuration was modelled with δ = 0° to 8° with C_L and L/D shown in Fig. 4a and b respectively. The results for the NACA0012 wing alone are predicted using the values from the CFD simulations that were compared to the Vortex-Lattice (VL) method provided by XFRL5 in [11].

C_L of the numerical simulations [11] compared to a wing alone at the same α = 6° shows that at δ = 4° the WBT provides the same lifting capabilities and at the same δ the L/D is at the maximum point in Fig. 4b. The existence of an ideal δ shown by the CFD results, might suggest that there is a unique aftbody deflection for a given KE shape. The CFD results also suggest that there exists some threshold δ where the WBT would be more efficient than a wing alone, and that the KE can be used as a high-lift device, and so the question posed is whether this would be a global optimum or whether it would be unique for each KE shape and for every different body.

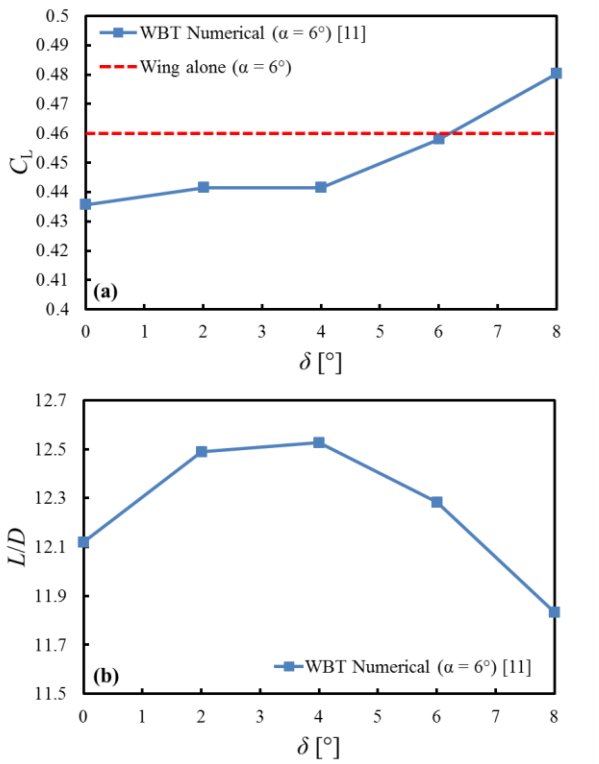

Fig. 4. Variation of a) C_L and b) L/D with δ for the WBT. Adapted from [11]

3.2.2 KE and aftbody geometry optimisation

The KE geometry (T_S and T_L/l) is varied with δ and L/D is estimated for 50 different simulations. From [12] it was expected that T_S would reduce to a small angle so as to avoid the KE interacting with the freestream outside the wake of the body. The wake diameter was assumed to be 10% of the body length based on experiments on seven different body shapes that were tested at Re on the order of 10^6 [17]. This assumption leads to a wake diameter estimate of 0.032m, resulting in an estimated ideal T_S < 17°.

Fig. 5 compares the KE geometry variables to the L/D values. L/D is less affected by the T_L/l changes, and for a given T_S there is a prescribed T_L/l. A shorter, narrower KE would lead to the best L/D with T_S = 4°, which is well

within the predicted T_S range, based on the wake diameter.

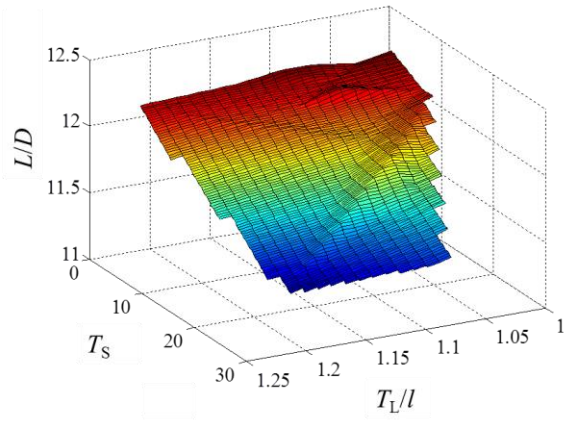

Fig. 5. L/D as a function of to T_S and T_L/l for the WBT

Comparing δ to T_S in Fig. 6 in terms of L/D, a specific T_S does not show much variation in δ but that a $T_S < 12°$ is preferred to maximise L/D. A general guideline can therefore be assumed that for any δ a shorter, narrower KE would offer a better overall L/D and that the design is more sensitive to T_S variation compared to both T_L/l and δ.

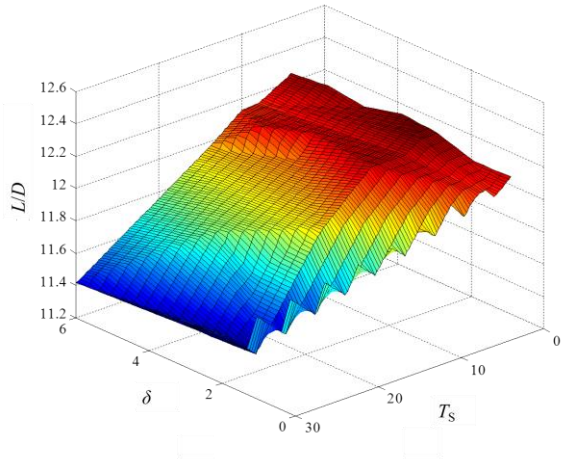

Fig. 6. L/D as a function of to T_S and δ for the WBT

Figure 7a indicates the percentage increase in C_L to be greater than that of a NACA0012 wing alone at $\alpha = 6°$ for the WBT at different T_S and δ. The dark blue regions indicate a design space where the WBT can provide the same C_L as the wing alone and for all other colours, the aftbody deflections and KE shape can be used as a high-lift device. Again for $T_S < 12°$ there is hardly any sensitivity to δ, however as T_S increases, δ has a larger impact and should be optimised.

In [12] it is concluded that for an ideal combination of LDB-KE the KE will remain within the bounds of the viscous wake, which is confirmed by Fig. 7a. A larger T_S increases the sensitivity of T_L/l and δ since they will lead to either a larger portion of the KE outside of the viscous wake or at a larger local angle, leading to a reduced L/D.

For the majority of the 50 cases there is an average of 3% increase in C_L compared to the wing alone at $\alpha = 6°$ as shown in Fig. 7b. There are a couple of exceptions where the C_L is 5% or more but at a drag penalty shown by the reduction in L/D compared to the optimum case.

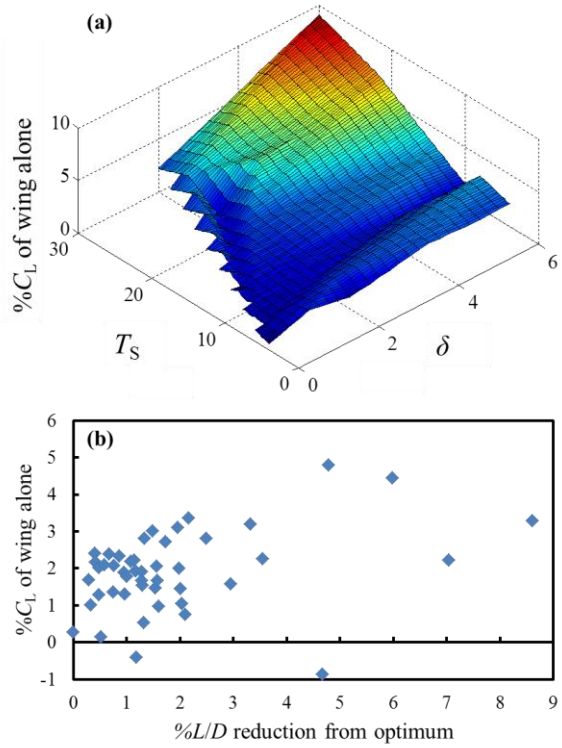

Fig. 7. a) The percentage increase of C_L for the WBT compared to the wing alone for a) different T_S and δ and b) the percentage variance in L/D from the original WBT [9-11] compared to the optimised case

The results from Fig. 7 show the potential of the WBT to contribute to lift and in restoring a more uniform downwash distribution, there is further the possibility of reducing α of the wing, which would lead to a drag reduction of the overall configuration. A small immediate penalty in L/D shown by Fig. 7b, could be

rectified by adjusting α, but at different α there could be a different sensitivity in T_S, T_L/l and δ.

3.3 Discussion of results

Initial results [10, 11] suggest that for a constant T_S and T_L/l there is a unique and optimal δ, but this was found in this optimisation study. Even though L/D was maximised in each case the sensitivities to the varying parameters were not as great as [10, 11] suggested.

The optimisation simulations (varying T_S, T_L/l and δ) showed that at a specific α, the WBT is fairly insensitive to variations in δ when T_S and T_L/l is optimised for a maximum L/D. The ideal KE geometry requires a reduced T_S and T_L/l from the initial case, with a final optimised $L/D = 12.4$ for $T_S = 4°$ and $T_L/l = 1.08$ at $\delta = 2°$.

The purpose of the KE is not primarily to add lift to the wing alone, but to recover the lift lost due to the presence of the body. The results suggest that for an ideal WBT, the KE as a discrete flat plate deflector flap can recover the lost lift as well as increase the total, but there is a penalty in drag. Primarily the drag penalty is due to the pressure drag [12] which increases with increasing δ due to the increase of the effective base area of the aftbody. For a KE with higher T_S, the base area increases with increasing δ, explaining the sensitivity to T_S.

4 Low drag bodies with WBT configuration

4.1 Optimisation with F-57

The F-57 LDB was selected from [12] and used to evaluate the impact of a LDB geometry and pressure recovery on a WBT configuration. Another 50 simulations were completed with the F-57 LDB. Figure 8 shows the KE geometry parameters, T_S and T_L/l with the estimated L/D of the F-57. The same trend was observed as for the WBT where T_S is the sensitive design variable.

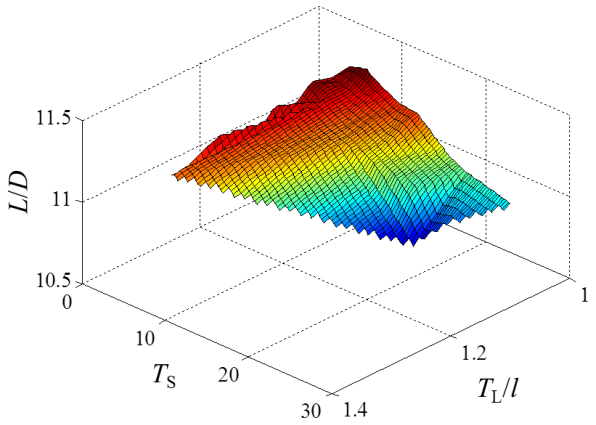

Fig. 8. L/D as a function of T_S and T_L/l for the F-57

The influence of T_S and δ is also the same for the two configurations, with a decrease in L/D as T_S is increased and a smaller sensitivity to δ (Fig. 9).

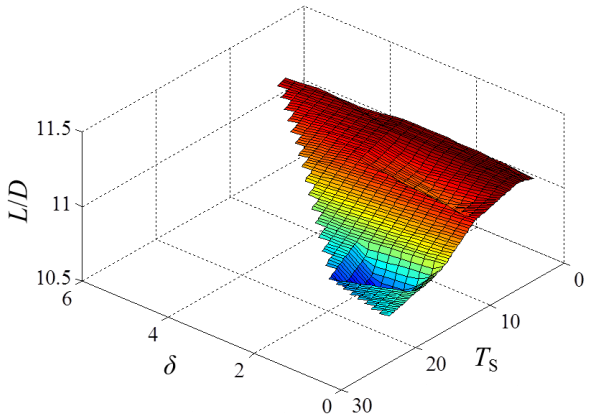

Fig. 9. L/D as a function of T_S and δ for the F-57

Figure 10a shows the same trend as for the WBT, where for $T_S < 12°$, the δ is not a sensitive design variable but as T_S increases δ will have to be adjusted. The F-57 shows a reduction in C_L from the wing alone in all the simulated cases as shown in Fig. 10b. In contrast to the WBT the F-57 does not restore the downwash distribution but shows a significant decrease in C_L.

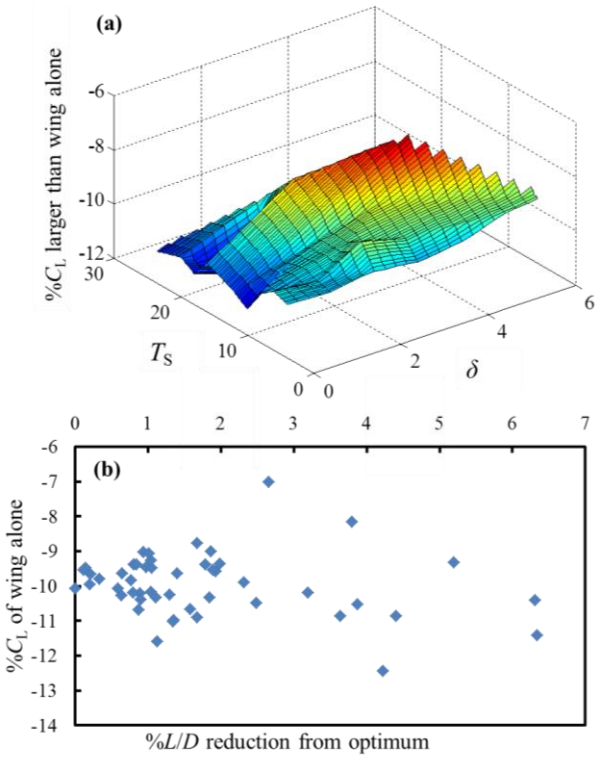

Fig. 10. a) The percentage reduction of C_L for the WBT compared to the wing alone for a) different T_S and δ and b) the percentage variance in L/D from the F-57 compared to the optimised case

4.2 WBT and F-57 Comparison

The optimisation simulation using the F-57 has an optimum of L/D = 11.3 for T_S = 4° and T_L/l = 1.08 at δ = 2° which has the same KE shape and aftbody deflection as for the WBT without the LDB but at a 9% reduction of overall L/D. The reason for this reduction was due to a reduction of lift as well as an increase in drag for the F-57.

Figure 11 shows the spanwise distribution of the vertical velocity component for the WBT and the F-57, where the F-57 is providing less lift than the more bluff aftbody WBT, similar to the findings in [12] for the LDB-KEs alone. This might suggest that the Myring LDB investigated in [12] might produce an improvement in L/D, by reducing the overall drag rather than the F-57 LDB, since the Myring LDB has a more bluff aftbody, similar to the WBT body.

The purpose of the LDB is to reduce the drag of the body with the prospect of an overall further reduction in drag for the WBT. However, with the addition of the KE the flow separation over the aftbody of the F-57 is substantially more than for the WBT. Figure 12 shows a normalised streamwise wake velocity profile at x/l = 1.08 for the F-57 and the WBT, where it is shown that the wake diameter and defect magnitude are both larger, leading to a larger pressure drag component for the F-57.

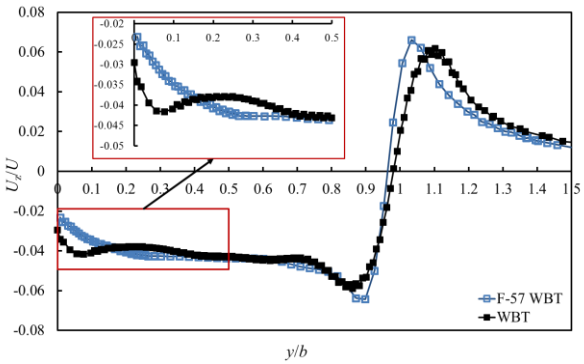

Fig. 11. Vertical velocity component U_z/U as a function of spanwise normalised by wing span y/b, at location x/l = 1.08 for WBT and F-57 at the optimum cases (T_S = 4°, T_L/l = 1.08 and δ = 2°)

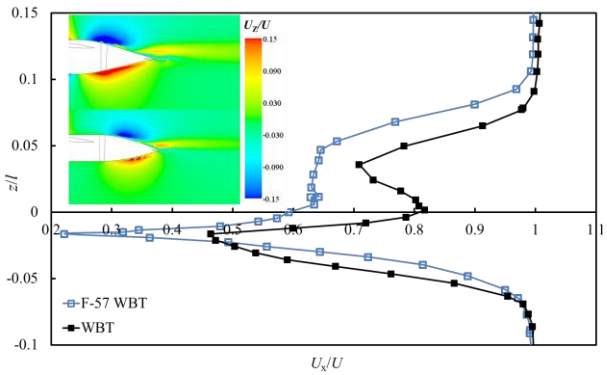

Fig. 12. Normalised streamwise wake velocity profiles for WBT and F-57 optimum cases (T_S = 4°, T_L/l = 1.08 and δ = 2°). Insert shows the relative velocity magnitude contours on the symmetry plane in the wake region.

5 Conclusions and final remarks

The optimisation algorithm SHERPA was used to search 50 different aftbody deflections and KE geometries of a WBT with a fixed wing for the variation in total L/D. A second set of 50 simulations was conducted, where the F-57 LDB replaced the conventional body in the WBT. In both cases, the optimum seemed to point to T_S as the most sensitive design variable, with T_L/l and δ only becoming important at T_S > 12°.

The replacement of the conventional body with the F-57 LDB does not prove to reduce the overall drag but rather causes an overall decrease in efficiency due to a reduced ability to provide lift and an increase in drag due to increased separation over the aftbody. However, the results suggest that a more bluff body in the WBT could provide a design space where the drag can be reduced and by a slight deflection and a short narrow KE can improve the overall efficiency. Most importantly, the aftbody and KE should not be designed in isolation but rather as a single continuous aftbody-KE unit.

Acknowledgments

The authors would like to thank the South African National Aerospace Center (NAC) and Airbus for their financial support with this research project.

References

[1] Agenbag DS, Theron NJ and Huyssen RJ. Pitch handling qualities investigation of the tailless gull-wing configuration. *Journal of Aircraft*, Vol. 46, No. 2, pp. 683-691, 2009.

[2] Carmichael BH. Underwater vehicle drag reduction through choice of shape. *AIAA Paper 66-657*, 1966.

[3] Lutz T and Wagner S. Drag reduction and shape optimization of airship. *Journal of Aircraft*, Vol. 35, No. 3, pp. 345-351, 1998.

[4] Li Y, Nahon M and Sharf I. Airship dynamics modeling: A literature review. *Progress in Aerospace Science*, Vol. 47, pp. 217-239, 2011.

[5] Parsons JS and Goodson RE. Optimum shaping of axisymmetric bodies for minimum drag in incompressible flow. Ph.D Dissertation, Purdue University, Lafayette, Ind, 1972.

[6] Myring DF. The profile drag of bodies of revolution in subsonic axisymmetric flow. *Royal Aircraft Est*, TR72234, 1972.

[7] Myring DF. A theoretical study of the effects of body shape and Mach number on the drag bodies of revolution in subcritical axisymmetric flow. *Royal Aircraft Est*, TR8100, 1981.

[8] Krauss ES. Effect of shapes of conventional fuselages and of streamlined bodies on drag at subsonic speeds. *Zeitscrift fur flugwissenschaft und weltraumforschung*, Vol. 16, pp. 429-438, 1968.

[9] Huyssen RJ, Spedding GR, Mathews EH and Liebenberg L. Wing-body circulation control by means of a fuselage trailing edge. *Journal of Aircraft*, Vol. 49, No. 5, pp. 1279-1289, 2012.

[10] Davis TW and Spedding GR. Lift and drag measurements of a Gull-wing configuration aircraft. *53rd AIAA Aerospace Sciences Meeting*, Kissimmee, FL, USA, AIAA 2015-0027, 2015.

[11] Smith L, Meyer JP and Spedding GR. Numerical simulations of a proposed wing-body-tail configuration. *54rd AIAA Aerospace Sciences Meeting*, San Diego, CA, USA, AIAA 2016-0800, 2016.

[12] Smith L, Craig KJ, Meyer, JP and Spedding GR. Modifying low-drag bodies to generate lift: a computational study. *Unpublished*, 2016.

[13] ASME V&V 20. Standard for verification and validation in computational fluid dynamics and heat transfer. *American Society of Mechanical Engineers*, 2009.

[14] Menter FR. Two-Equation eddy-viscosity turbulence models for engineering applications. *AIAA Journal*, Vol. 32, No. 8, pp. 1598-1605, 1994.

[15] Langtry RB. A Correlation-Based transition model using local variables for unstructured parallelized CFD codes. Ph.D Dissertation, University of Stuttgart, 2006.

[16] Chase N, Rademacher M, Goodman E, Averill R, and Sidhu R. A benchmark study of optimization search algorithms. *Red Cedar Technology*. BMK-3022 Rev. 01.10.

[17] Patel VC and Chen HC. Flow over tail and in wake of axisymmetric bodies: Review of the state of the art. *Journal of ship research*, Vol. 30, No. 3, pp. 201-214, 1986.

6 Contact Author Email Address

Mailto: Lelanie.smith@up.ac.za

Copyright Statement